

A description of pseudorapidity distributions of charged particles produced in Au+Au collisions at RHIC energies

Z. J. Jiang^{*}, Dongfang Xu, and Yan Huang

College of Science, University of Shanghai for Science and Technology, Shanghai 200093, China

**jzj265@163.com*

The charged particles produced in heavy ion collisions consist of two parts: One is from the freeze-out of hot and dense matter formed in collisions. The other is from the leading particles. In this paper, the hot and dense matter is assumed to expand according to the hydrodynamic model including phase transition and decouples into particles *via* the prescription of Cooper-Frye. The leading particles are as usual supposed to have Gaussian rapidity distributions with the number equaling that of participants. The investigations of this paper show that, unlike low energy situations, the leading particles are essential in describing the pseudorapidity distributions of charged particles produced in high energy heavy ion collisions. This might be due to the different transparencies of nuclei at different energies.

Keywords: relativistic hydrodynamics; phase transition; pseudorapidity distribution

PACS Number(s): 25.75.Ag, 25.75.Ld, 25.75.Dw, 13.85.-t

1. Introduction

The BNL Relativistic Heavy Ion Collider (RHIC) accelerates nuclei up to the center-of-mass energies from a dozen GeV to 200 GeV per nucleon. In the past decade, the measurements from such collisions have triggered an extensive research for the properties of matter at extreme conditions of very high temperature and energy densities [1-33]. One of the most important achievements from such research is the discovery that the matter created in nucleus-nucleus collisions at RHIC energies is in the state of strongly coupled quark-gluon plasma (sQGP) exhibiting a clear collective behavior nearly like a perfect fluid with very low viscosity [10-33].

The best approach for describing the space-time evolution of fluid-like sQGP is the relativistic hydrodynamics, which was first put forward by L. D. Landau in his pioneering work in 1953 [34].

However, since the partial differential equations of relativistic hydrodynamics are highly nonlinear, it is a formidable task to solve them analytically. This is the reason why, from the time of Landau until now, the exact solutions of relativistic hydrodynamics are mainly limited to 1+1 expansion for a perfect fluid with simple equation of state. To solve the equations of high-dimensional expansions especially for situations incorporating the effect of viscosities or pressure anisotropies, one has to resort to the means of computer simulations.

One of the most important applications of 1+1 dimensional hydrodynamics is the analysis of the pseudorapidity distributions of charged particles in high energy physics. In this paper, combining the effect of leading particles, we will discuss such distributions in the framework of hydrodynamic model including phase transition [10]. In section 2, a brief introduction is given to the theoretical model, presenting its exact solutions. The solutions are then used in section 3 to formulate the pseudorapidity distributions of charged particles resulted from the freeze-out of sQGP. Together with the contribution from leading particles, the results are then compared with the experimental observations performed by PHOBOS Collaboration at RHIC in Au+Au collisions at $\sqrt{s_{NN}}=200$ and 19.6 GeV [5], respectively. The last section 4 is traditionally about conclusions.

2. A brief introduction to the model

Here, for the purpose of completeness and applications, we will list the key ingredients of the hydrodynamic model [10].

(1) The movement of fluid follows the continuity equation

$$\frac{\partial T^{\mu\nu}}{\partial x^\nu} = 0, \quad \mu, \nu = 0, 1, \quad (1)$$

where $x^\nu = (x^0, x^1) = (t, z)$, t is the time and z is the longitudinal coordinate along beam direction.

$T^{\mu\nu}$ is the energy-momentum tensor, which, for a perfect fluid, takes the form

$$T^{\mu\nu} = (\varepsilon + p)u^\mu u^\nu - pg^{\mu\nu}, \quad (2)$$

where $g^{\mu\nu} = g_{\mu\nu} = \text{diag}(1, -1)$ is the metric tensor.

$$u^\mu = (u^0, u^1) = (\cosh y_F, \sinh y_F), \quad u^\mu u_\mu = 1, \quad (3)$$

is the 4-velocity of fluid, y_F is its rapidity. ε and p in Eq. (2) are the energy density and

pressure of fluid, which meet the thermodynamical relations

$$\varepsilon + p = Ts, \quad d\varepsilon = Tds, \quad dp = sdT, \quad (4)$$

where T and s are the temperature and entropy density of fluid, respectively. To close Eq. (1), another relation, namely the equation of state

$$\frac{dp}{d\varepsilon} = \frac{sdT}{Tds} = c_s^2 \quad (5)$$

is needed, where c_s is the sound speed of fluid, which takes different values in sQGP and in hadronic phase.

(2) Project Eq. (1) to the direction of u_μ and the direction perpendicular to u_μ , respectively.

This leads to equations

$$\frac{\partial(su^\nu)}{\partial x^\nu} = 0, \quad (6)$$

$$\frac{\partial(T \sinh y_F)}{\partial t} + \frac{\partial(T \cosh y_F)}{\partial z} = 0. \quad (7)$$

Eq. (6) is the continuity equation for entropy conservation. Eq. (7) means the existence of a scalar function ϕ satisfying relations

$$\frac{\partial\phi}{\partial t} = T \cosh y_F, \quad \frac{\partial\phi}{\partial z} = -T \sinh y_F. \quad (8)$$

From ϕ and Legendre transformation, Khalatnikov potential χ is introduced *via* relation

$$\chi = \phi - tT \cosh y_F + zT \sinh y_F. \quad (9)$$

In terms of χ , the variables t and z can be expressed as

$$\begin{aligned} t &= \frac{e^\theta}{T_0} \left(\frac{\partial\chi}{\partial\theta} \cosh y_F + \frac{\partial\chi}{\partial y_F} \sinh y_F \right), \\ z &= \frac{e^\theta}{T_0} \left(\frac{\partial\chi}{\partial\theta} \sinh y_F + \frac{\partial\chi}{\partial y_F} \cosh y_F \right), \end{aligned} \quad (10)$$

where T_0 is the initial temperature of fluid and $\theta = \ln(T_0/T)$. Through above equations, the coordinate base of (t, z) is transformed to that of (θ, y_F) , and Eq. (6) is translated into the so called telegraphy equation

$$\frac{\partial^2 \chi}{\partial \theta^2} - 2\beta \frac{\partial \chi}{\partial \theta} - \frac{1}{c_s^2} \frac{\partial^2 \chi}{\partial y_F^2} = 0, \quad \beta = \frac{1 - c_s^2}{2c_s^2}. \quad (11)$$

(3) Along with the expansions of matter created in collisions, it becomes cooler and cooler. As its temperature drops from the initial T_0 to the critical T_c , phase transition occurs. The matter transforms from sQGP state to hadronic state. The produced hadrons are initially in the violent and frequent collisions. The major part of these collisions is inelastic. Hence, the abundances of identified hadrons are in changing. Furthermore, the mean free paths of these primary hadrons are very short. The movement of them is still like that of a fluid meeting Eq. (11) with only difference being the value of c_s . In sQGP, $c_s = c_0 = 1/\sqrt{3}$, which is the sound speed of a massless perfect fluid, being the maximum of c_s . In the hadronic state, $c_s = c_h < c_0$. At the point of phase transition, that is as $T = T_c$, c_s is discontinuous.

(4) The solution of Eq. (11) for the sector of sQGP is [10]

$$\chi_0(\theta, y_F) = \frac{q_0 c_0}{2} e^{\beta_0 \theta} I_0 \left(\beta_0 c_0 \sqrt{y_0^2(\theta) - y_F^2} \right), \quad (12)$$

where q_0 is a constant determined by tuning the theoretical results to experimental data. I_0 is the 0th order modified Bessel function of the first kind, and

$$\beta_0 = \frac{1 - c_0^2}{2c_0^2} = 1, \quad y_0(\theta) = \frac{\theta}{c_0}. \quad (13)$$

In the sector of hadrons, the solution of Eq. (11) is [10]

$$\chi_h(\theta, y_F) = \frac{q_0 c_0}{2} B(\theta) I_0 \left[\lambda(\theta, y_F) \right], \quad (14)$$

where

$$B(\theta) = e^{\beta_h(\theta - \theta_c) + \beta_0 \theta_c}, \quad \lambda(\theta, y_F) = \beta_h c_h \sqrt{y_h^2(\theta) - y_F^2}, \quad (15)$$

$$\beta_h = \frac{1 - c_h^2}{2c_h^2}, \quad y_h(\theta) = \frac{\theta - \theta_c}{c_h} + \frac{\theta_c}{c_0}, \quad \theta_c = \ln \left(\frac{T_0}{T_c} \right).$$

3. The pseudorapidity distributions of charged particles

(1) The invariant multiplicity distributions of charged particles frozen out from sQGP

From Khalatnikov potential χ , the rapidity distributions of charged particles frozen out from fluid-like sQGP read [35]

$$\frac{dN_{\text{sQGP}}}{dy_F} = \frac{q_0 c_0}{2} A(b) \left(\cosh y \frac{dz}{dy_F} - \sinh y \frac{dt}{dy_F} \right), \quad (16)$$

where $A(b)$ is the area of overlap region of collisions, being the function of impact parameter b or centrality cuts. Inserting Eq. (10) into above equation, the part in the round brackets becomes

$$\begin{aligned} & \cosh y \frac{dz}{dy_F} - \sinh y \frac{dt}{dy_F} \\ &= \frac{1}{T} c^2 \frac{\partial}{\partial \theta} \left(\chi + \frac{\partial \chi}{\partial \theta} \right) \cosh(y - y_F) - \frac{1}{T} \frac{\partial}{\partial y_F} \left(\chi + \frac{\partial \chi}{\partial \theta} \right) \sinh(y - y_F). \end{aligned} \quad (17)$$

With the expansions of hadronic matter, it continues becoming cooler. According to the prescription of Cooper-Frye [35], as the temperature drops to the freeze-out temperature T_{FO} , the inelastic collisions among hadrons cease. The yields of identified hadrons maintain unchanged becoming the measured results in experiments. The invariant multiplicity distributions of charged particles equal [10, 15, 35]

$$\frac{d^2 N_{\text{sQGP}}}{2\pi p_T dy dp_T} = \frac{1}{(2\pi)^3} \int \frac{dN_{\text{sQGP}}}{dy_F} \frac{m_T \cosh(y - y_F)}{\exp\{[m_T \cosh(y - y_F) - \mu_B]/T\} + \delta} \Big|_{T=T_{\text{FO}}} dy_F, \quad (18)$$

where $m_T = \sqrt{m^2 + p_T^2}$ is the transverse mass of produced charged particle with rest mass m . μ_B in Eq. (18) is the baryochemical potential. For Fermi charged particles, $\delta=1$ in the denominator of Eq. (18), and for Bosons, $\delta=-1$. The meaning of Eq. (18) is evident. It is the convolution of dN_{sQGP}/dy_F with the energy of the charged particles in the state with temperature T .

The integral interval of y_F in Eq. (18) is $[-y_h(\theta_f), y_h(\theta_f)]$. The integrand is evaluated with $T=T_{\text{FO}}$. At this moment, the fluid freezes out into the charged particles. Replacing χ in Eq. (17) by χ_h of Eq. (14), it becomes

$$\begin{aligned} & \left(\cosh y \frac{dz}{dy_F} - \sinh y \frac{dt}{dy_F} \right) \Big|_{T=T_{\text{FO}}} \\ &= \frac{1}{T_{\text{FO}}} (\beta_h c_h)^2 B(\theta_{\text{FO}}) [S(\theta_{\text{FO}}, y_F) \sinh(y - y_F) + C(\theta_{\text{FO}}, y_F) \cosh(y - y_F)], \end{aligned} \quad (19)$$

where

$$S(\theta_{FO}, y_F) = \frac{\beta_h y_F}{\lambda(\theta_{FO}, y_F)} \left\{ \frac{\beta_h c_h y_h(\theta_{FO})}{\lambda(\theta_{FO}, y_F)} I_0[\lambda(\theta_{FO}, y_F)] \right. \\ \left. + \left[\frac{\beta_h + 1}{\beta_h} - \frac{2\beta_h c_h y_h(\theta_{FO})}{\lambda^2(\theta_{FO}, y_F)} \right] I_1[\lambda(\theta_{FO}, y_F)] \right\}, \quad (20)$$

$$C(\theta_{FO}, y_F) = \left\{ \frac{\beta_h + 1}{\beta_h} + \frac{[\beta_h c_h y_h(\theta_{FO})]^2}{\lambda^2(\theta_{FO}, y_F)} \right\} I_0[\lambda(\theta_{FO}, y_F)] \\ + \frac{1}{\lambda(\theta_{FO}, y_F)} \left\{ \frac{y_h(\theta_{FO})}{c_h} + 1 - \frac{2[\beta_h c_h y_h(\theta_{FO})]^2}{\lambda^2(\theta_{FO}, y_F)} \right\} I_1[\lambda(\theta_{FO}, y_F)], \quad (21)$$

where I_1 is the 1st order modified Bessel function of the first kind.

(2) The invariant multiplicity distributions of leading particles

It is believed that the leading particles are formed outside the nucleus, that is, outside the colliding region [36, 37]. The generation of leading particles is therefore free from fluid evolution. Hence, their rapidity distributions are beyond the scope of hydrodynamic description and should be treated separately.

In our previous work [24-26], we once argued that the rapidity distributions of leading particles take the Gaussian form

$$\frac{dN_{\text{Lead}}(b, \sqrt{s_{\text{NN}}}, y)}{dy} = \frac{N_{\text{Lead}}(b, \sqrt{s_{\text{NN}}})}{\sqrt{2\pi}\sigma} \exp \left\{ -\frac{[|y| - y_0(b, \sqrt{s_{\text{NN}}})]^2}{2\sigma^2} \right\}, \quad (22)$$

where $y_0(b, \sqrt{s_{\text{NN}}})$ is the central position of distributions, which should increase with incident energies and centrality cuts. σ in Eq. (22) is the width of distributions, which should not, at least not apparently, depend on the incident energies, centrality cuts and even colliding systems. Both y_0 and σ can be determined by tuning the theoretical predictions to experimental data.

$N_{\text{Lead}}(b, \sqrt{s_{\text{NN}}})$ in Eq. (22) is the number of leading particles, which, for an identical nucleus-nucleus collision, equals half of the number of participants.

The investigations have shown that [38], for certain rapidity, the invariant multiplicity distributions of leading particles possess the form

$$\frac{d^2 N_{\text{lead}}}{2\pi p_T dy dp_T} \propto \exp(-ap_T^2), \quad (23)$$

where a is a constant. Then, as a function of rapidity, the invariant multiplicity distributions of leading particles can be written as

$$\frac{d^2 N_{\text{lead}}}{2\pi p_T dy dp_T} = \frac{dN_{\text{Lead}}}{dy} \frac{a}{\pi} \exp(-ap_T^2), \quad (24)$$

which is normalized to N_{lead} .

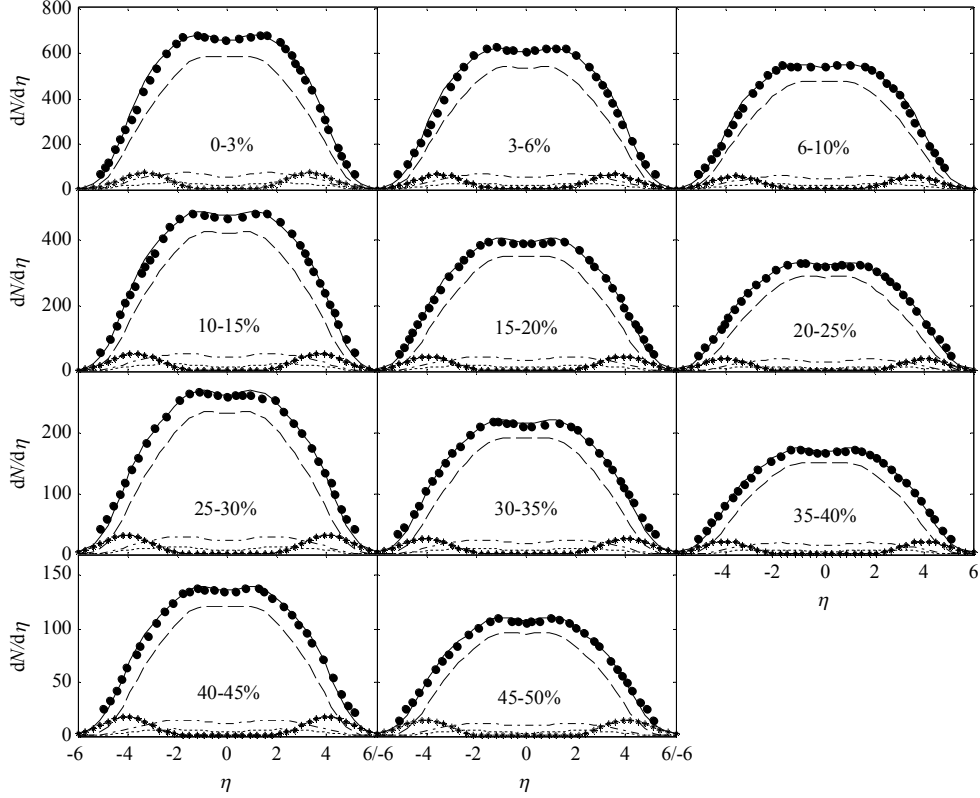


FIGURE 1: The pseudorapidity distributions of charged particles produced in different centrality Au+Au collisions at $\sqrt{s_{\text{NN}}} = 200$ GeV. The dashed, dashed-dotted and dotted curves are respectively the contribution from pions, kaons and protons got from the hydrodynamic result of Eq. (18). The dotted-star curves are the components of leading particles obtained from Eq. (24). The solid curves are the sums of the four types of curves.

(3) The pseudorapidity distributions of charged particles

Writing invariant multiplicity distributions in terms of pseudorapidity, we have

$$\frac{d^2 N}{2\pi p_T d\eta dp_T} = \sqrt{1 - \frac{m^2}{m_T^2 \cosh^2 y}} \frac{d^2 N}{2\pi p_T dy dp_T}, \quad (25)$$

where

$$\frac{d^2 N}{2\pi p_T dy dp_T} = \frac{d^2 N_{\text{sQGP}}}{2\pi p_T dy dp_T} + \frac{d^2 N_{\text{lead}}}{2\pi p_T dy dp_T}. \quad (26)$$

To fulfill the transformation of Eq. (25), another relation

$$y = \frac{1}{2} \ln \left[\frac{\sqrt{p_T^2 \cosh^2 \eta + m^2} + p_T \sinh \eta}{\sqrt{p_T^2 \cosh^2 \eta + m^2} - p_T \sinh \eta} \right] \quad (27)$$

is in order.

Substituting Eqs. (18) and (24) into Eq.(25) and carrying out the integration of p_T , we can get the pseudorapidity distributions of charged particles produced in high energy heavy ion collisions. Figure 1 shows such distributions in Au+Au collisions at $\sqrt{s_{NN}} = 200$ GeV. The solid dots in the figure are the experimental measurements [5]. The dashed, dashed-dotted and dotted curves are respectively the contribution from pions, kaons and protons got from the hydrodynamic result of Eq. (18). The dotted-star curves are the components of leading particles obtained from Eq. (24). The solid curves are the sums of the four types of curves. The χ^2/NDF for each curve is listed in Table 1. It can be seen that the combined contribution from both hydrodynamics and leading particles matches up well with experimental data.

Table 1: The χ^2/NDF , initial temperature T_0 and central position y_0 in different centrality Au+Au collisions at $\sqrt{s_{NN}} = 200$ and 19.6 GeV, respectively.

Centrality cuts (%)		0-3	3-6	6-10	10-15	15-20	20-25	25-30	30-35	35-40	40-45	45-50
χ^2/NDF	200 GeV	0.496	0.693	0.402	0.260	0.310	0.217	0.354	0.151	0.161	0.123	0.089
	19.6 GeV	0.816	0.533	0.359	0.614	0.802	0.309	0.559	0.496	0.229	0.577	---
$T_0(\text{GeV})$	200 GeV	0.950	0.949	0.948	0.947	0.945	0.941	0.922	0.909	0.885	0.874	0.860
	19.6 GeV	0.551	0.549	0.547	0.543	0.539	0.533	0.529	0.518	0.510	0.493	---
y_0		2.86	3.03	3.13	3.23	3.46	3.54	3.55	3.57	3.58	3.59	3.60

Experiments have shown that the overwhelming majority of charged particles produced in Au+Au collisions at $\sqrt{s_{NN}} = 200$ GeV consists of pions, kaons and protons with proportions of about 84%, 12% and 4%, respectively [39], which are roughly independent of energies, centrality cuts and colliding systems. In calculations, the ratios of these three kinds of particles take about the same as these values. T_c in Eq. (15) takes the well-recognized value of $T_c = 180 \text{ MeV}$. c_h in Eq. (15) takes the value of $c_h = 0.45$ from the investigations of Refs. [15, 40-42]. The freeze-out temperature T_{FO} takes the values of $T_{FO} = 120 \text{ MeV}$ from the studies of Ref. [6], which also

shows that the baryochemical potential μ_b in Eq. (18) is about equal to 20 MeV. For the most central collisions, T_0 in Eq. (15) takes the value of $T_0 = 0.95$ referring to that given in Ref. [15]. This allows us to determine the constant q_0 in Eq. (16) to be $q_0 = 7.38 \times 10^{-4}$, 6.01×10^{-4} and 4.50×10^{-3} for pions, kaons and protons, respectively. Keeping q_0 unchanged, T_0 is fixed for the rest centrality cuts by making theoretical results fit in with experimental data. The results are listed in Table 1. It can be seen that T_0 decreases slowly with increasing centralities especially in the first four cuts. Table 1 also lists the central position y_0 in Eq. (22). As addressed above, it increases with increasing centralities. The width parameter σ in Eq. (22) values a constant of $\sigma = 0.90$, being independent of centrality cuts. The parameter a in Eq. (24) takes the value of $a = 0.92$.

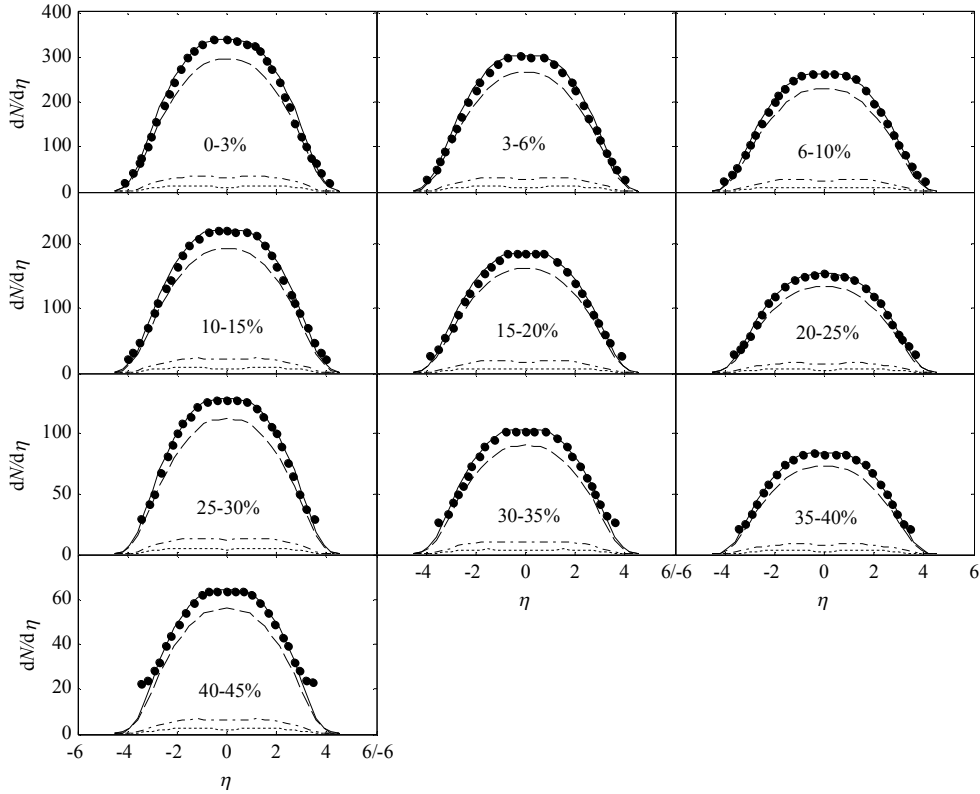


FIGURE 2: The pseudorapidity distributions of charged particles produced in different centrality Au+Au collisions at $\sqrt{s_{NN}} = 19.6$ GeV. The dashed, dashed-dotted and dotted curves are respectively the contribution from pions, kaons and protons got from the hydrodynamic results of Eq. (18). The solid curves are the sums of the three types of curves.

Figure 2 shows the pseudorapidity distributions of charged particles produced in Au+Au

collisions at $\sqrt{s_{\text{NN}}} = 19.6 \text{ GeV}$. The χ^2/NDF for each curve is listed in Table 1. The meanings of different types of curves are the same as those in Figure 1. It can be seen that, in the absence of leading particles, the hydrodynamics alone can give a good description to the experimental observations. This is different from Figure 1. Where, leading particles are essential in fitting experimental data. This difference might be caused by the different transparencies of nuclei in different energies. As the analyses given in Ref. [43], in central Au+Au collisions at $\sqrt{s_{\text{NN}}} = 200 \text{ GeV}$, the leading particles locate at about $y_0 = 2.91$. This position is far away from the mid-rapidity region. Where, relative to the low yields of charged particles frozen out from sQGP, the effect of leading particles is evident which should be considered separately. On the contrary, in case of Au+Au collisions at $\sqrt{s_{\text{NN}}} = 19.6 \text{ GeV}$, $y_0 = 1.28$. This position is so close to the mid-rapidity region that the effect of leading particles is hidden by the large yields of charged particles generated from the freeze-out of sQGP. Therefore, there is no need to consider the contribution of leading particles separately.

In drawing Figure 2, T_0 takes the values as those listed in Table 1. $c_h = 0.40$ and $\mu_B = 210 \text{ MeV}$. The other parameters, such as T_c , T_{FO} and q_0 are the same as those used in drawing Figure 1.

4. Conclusions

By taking into consideration the effect of leading particles, the hydrodynamic model incorporating the phase transition is used to analyze the pseudorapidity distributions of charged particles produced in Au+Au collisions at RHIC energies.

The hydrodynamic model contains a rich information about transport coefficients of sQGP, such as the sound speed c_0 in sQGP, the sound speed c_h in hadronic phase, the phase transition temperature T_c , the chemical freeze-out temperature T_{FO} , the baryochemical potential μ_B and the initial temperature T_0 . With the exception of T_0 , the other five coefficients take the values either from the well-known theoretical results or from experimental measurements. As for T_0 , there are no widely accepted results so far. In our calculations, T_0 in the most central Au+Au

collisions at $\sqrt{s_{\text{NN}}} = 200 \text{ GeV}$ takes the value referring to that given by other investigations, which enables us to ascertain the constant q_0 in Eq. (16). In the rest centrality cuts and in Au+Au collisions at $\sqrt{s_{\text{NN}}} = 19.6 \text{ GeV}$, T_0 is determined by maintaining q_0 unchanged and comparing the theoretical results with experimental data.

The leading particles, by conventional definition, are the particles carrying on the quantum numbers of colliding nucleons and taking away the most part of incident energy. They are separately in projectile and target fragmentation region. The present investigations show that the importance of leading particles in describing the pseudorapidity distributions of charged particles produced in heavy ion collisions is related to the incident energy. At high energy, owing to the high transparency of nuclei, the contribution of leading particles is evident and indispensable. While, at low energy, as a result of poor transparency of nuclei the effect of leading particles is integrated with the results of freeze-out of sQCD. It does not need to be dealt with separately.

Conflict of Interests

The authors declare that there is no conflict of interests regarding the publication of this paper.

Acknowledgments

This work is supported by the Shanghai Key Lab of Modern Optical System.

References

- [1] C. Adler and STAR Collaboration, "Measurement of inclusive antiprotons from Au+Au collisions at $\sqrt{s_{\text{NN}}} = 130 \text{ GeV}$," *Physical Review Letters*, vol. 87, Article ID 262302, 2001.
- [2] K. Adcox and PHENIX Collaboration, "Centrality dependence of $\pi^{+/-}$, $K^{+/-}$, p , and \bar{p} production from $\sqrt{s_{\text{NN}}} = 130 \text{ GeV}$ Au+Au collisions at RHIC," *Physical Review Letters*, vol. 88, Article ID 242301, 2002.
- [3] S. S. Adler and PHENIX collaboration, "Elliptic flow of identified hadrons in Au+Au collisions at $\sqrt{s_{\text{NN}}} = 200 \text{ GeV}$," *Physical Review Letters*, vol. 91, Article ID 182301, 2003.
- [4] K. Adcox and PHENIX Collaboration, "Single identified hadron spectra from $\sqrt{s_{\text{NN}}} = 130 \text{ GeV}$ Au+Au collisions," *Physical Review C*, vol. 69, Article ID 024904, 2004.
- [5] B. Alver and PHOBOS Collaboration, "Charged-particle multiplicity and pseudorapidity distributions measured with the PHOBOS detector in Au+Au, Cu+Cu, d+Au, and p+p collisions at ultrarelativistic energies," *Physical Review C*, vol. 83, Article ID 024913, 2011.

- [6] B. I. Abelev and STAR Collaboration, “Systematic measurements of identified particle spectra in $p+p$, $d+Au$, and $Au+Au$ collisions at the STAR detector,” *Physical Review C*, vol. 79, Article ID 034909, 2009.
- [7] A. Adare and PHENIX Collaboration, “Spectra and ratios of identified particles in $Au+Au$ and $d+Au$ collisions at $\sqrt{s_{NN}}=200$ GeV,” *Physical Review C*, vol. 88, Article ID 024906, 2013.
- [8] L. C. Arsene and BRAHMS collaboration, “Rapidity and centrality dependence of particle production for identified hadrons in $Cu+Cu$ collisions at $\sqrt{s_{NN}} = 200$ GeV,” *Physical Review C*, vol. 94, Article ID 014907, 2016.
- [9] L. Adamczyk and STAR Collaboration, “Centrality dependence of identified particle elliptic flow in relativistic heavy ion collisions at $\sqrt{s_{NN}}=7.7-62.4$ GeV,” *Physical Review C*, vol. 93, Article ID 014907, 2016.
- [10] N. Suzuki, “One-dimensional hydrodynamical model including phase transition,” *Physical Review C*, vol. 81, Article ID 044911, 2010.
- [11] A. Bialas, R. A. Janik, and R. Peschanski, “Unified description of Bjorken and Landau 1+1 hydrodynamics,” *Physical Review C*, vol. 76, Article ID 054901, 2007.
- [12] G. Beuf, R. Peschanski, and E. N. Saridakis, “Entropy flow of a perfect fluid in (1+1) hydrodynamics,” *Physical Review C*, vol. 78, no. 6, Article ID 064909, 2008.
- [13] T. Csörgo, M. I. Nagy, and M. Csanád, “New family of simple solutions of relativistic perfect fluid hydrodynamics,” *Physics Letters B*, vol. 663, pp. 306–311, 2008.
- [14] M. Csanád, M. I. Nagy, and S. Lökös, “Exact solutions of relativistic perfect fluid hydrodynamics for a QCD Equation of State,” *The European Physical Journal A*, vol. 48, pp. 173–178, 2012.
- [15] T. Mizoguchi, H. Miyazawa, and M. Biyajima, “A potential including the Heaviside function in the 1+1 dimensional hydrodynamics by Landau : Its basic properties and application to data at RHIC energies,” *European Physical Journal A*, vol. 40, no. 1, pp. 99–108, 2009.
- [16] T. S. Biró, “Analytic solution for relativistic transverse flow at the softest point,” *Physics Letters. B. Particle Physics, Nuclear Physics and Cosmology*, vol. 474, no. 1-2, pp. 21–26, 2000.
- [17] T. S. Biró, “Generating new solutions for relativistic transverse flow at the softest point,” *Physics Letters B*, vol. 487, pp. 133–139, 2000.
- [18] C. Y. Wong, “Landau hydrodynamics reexamined,” *Physical Review C*, vol. 78, Article ID 054902, 2008.
- [19] A. Bialas and R. Peschanski, “Asymmetric (1+1)-dimensional hydrodynamics in high-energy collisions,” *Physical Review C*, vol. 83, Article ID 054905, 2011.
- [20] E. K. G. Sarkisyan and A. S. Sakharov, “Relating multihadron production in hadronic and nuclear collisions,”

European Physical Journal C, vol. 70, no. 3, pp. 533–541, 2010.

- [21] C. Gale, S. Jeon, and B. Schenke, “Hydrodynamic modeling of heavy-ion collisions,” *International Journal of Modern Physics A*, vol. 28, Article ID 1340011, 2013.
- [22] U. Heinz and R. Snellings, “Collective flow and viscosity in relativistic heavy-ion collisions,” *Annual Review of Nuclear and Particle Science*, vol. 63, pp. 123–151, 2013.
- [23] A.N. Mishra, R. Sahoo, E. K. G. Sarkisyan, and A. S. Sakharov, “Effective-energy budget in multiparticle production in nuclear collisions,” *The European Physical Journal C*, vol. 74, p. 3147, 2014.
- [24] Z. J. Jiang, Q. G. Li, and H. L. Zhang, “Revised Landau hydrodynamic model and the pseudorapidity distributions of charged particles produced in nucleus-nucleus collisions at maximum energy at the BNL Relativistic Heavy Ion Collider,” *Physical Review C*, vol. 87, Article ID 044902, 2013.
- [25] Z. J. Jiang, Y. Zhang, H. L. Zhang, and H. P. Deng, “A description of the pseudorapidity distributions in heavy ion collisions at RHIC and LHC energies,” *Nuclear Physics A*, vol. 941, pp. 188–200, 2015.
- [26] Z. W. Wang, Z. J. Jiang, and Y. S. Zhang, “The investigations of pseudorapidity distributions of final multiplicity in Au+Au collisions at high energy,” *Journal of university of Shanghai for science and technology*, vol. 31, pp. 322–326, 2009 (in Chinese).
- [27] J. Qin and U. Heinz, “Hydrodynamic flow amplitude corrections in event-by-event fluctuating heavy-ion collisions,” *Physical Review C*, vol. 94, Article ID 024910, 2016.
- [28] E. K. G. Sarkisyan, A. N. Mishra, R. Sahoo, and A. S. Sakharov, “Multihadron production dynamics exploring the energy balance in hadronic and nuclear collisions,” *Physical Review D-Particles, Fields, Gravitation and Cosmology*, vol. 93, no. 7, Article ID 079904, 2016.
- [29] E. K. G. Sarkisyan, A. N. Mishra, R. Sahoo, and A. S. Sakharov, “Centrality dependence of midrapidity density from GeV to TeV heavy-ion collisions in the effective-energy universality picture of hadroproduction,” *Physical Review D*, vol. 94, Article ID 011501, 2016.
- [30] J. Noronha-Hostler, M. Luzum, and J.-Y. Ollitrault, “Hydrodynamic predictions for 5.02 TeV Pb-Pb collisions,” *Physical Review C-Nuclear Physics*, vol. 93, no. 3, Article ID 034912, 2016.
- [31] H. Niemi, K. J. Eskola, and R. Paatelainen, “Event-by-event fluctuations in a perturbative QCD+saturation+hydrodynamics model: Determining QCD matter shear viscosity in ultrarelativistic heavy-ion collisions,” *Physical Review C*, vol. 93, Article ID 024907, 2016.
- [32] F. G. Gardim, F. Grassi, M. Luzum, and J. Noronha-Hostler, “Hydrodynamic predictions for mixed harmonic correlations in 200 GeV Au+Au collisions,” *Physical Review C*, vol. 95, Article ID 034901, 2017.

- [33] M. Alqahtani, M. Nopoush, and M. Strickland, “Quasiparticle anisotropic hydrodynamics for central collisions,” *Physical Review C*, vol. 95, Article ID 034906, 2017.
- [34] L. D. Landau, “On the multiple production of particles in fast particle collisions,” *Izvestiya Akademii Nauk SSSR*, vol. 17, pp. 51–64, 1953 (Russian).
- [35] F. Cooper and G. Frye, “Landau’s hydrodynamic model of particle production and electron-positron annihilation into hadrons,” *Physical Review D*, vol. 11, pp. 192–213, 1975.
- [36] A. Berera, M. Strikman, W. S. Toothacker, W. D. Walker and J. J. Whitmore, “The limiting curve of leading particles from hadron-nucleus collisions at infinite A ,” *Phys. Lett. B*, vol. 403, pp. 1–7, 1997.
- [37] J. J. Ryan, *Proceeding of annual meeting of the division of particles and fields of the APS*, World Scientific, Singapore, 1993.
- [38] A. E. Brenner, D. C. Carev, and J. E. Elias et al., “Experimental study of single-particle inclusive hadron scattering and associated multiplicities,” *Physical Review D*, vol. 26, pp. 1497-1553, 1982.
- [39] S. S. Adler and PHENIX collaboration, “Identified charged particle spectra and yields in Au+Au collisions at $\sqrt{s_{NN}}=200$ GeV,” *Physical Review C*, vol. 69, Article ID 034909, 2004.
- [40] A. Adare and PHENIX Collaboration, “Scaling properties of azimuthal anisotropy in Au+Au and Cu+Cu collisions at $\sqrt{s_{NN}}=200$ GeV,” *Physical Review Letters*, vol. 98, Article ID 162301, 2007.
- [41] L. N. Gao, Y. H. Chen, H. R. Wei, and F. H. Liu, “Speed of sound parameter from RHIC and LHC heavy-ion data,” *Advances in High Energy Physics*, vol. 2014, Article ID 450247, 2014.
- [42] S. Borsányi, G. Endrodi, and Z. Fodor et al., “The QCD equation of state with dynamical quarks,” *Journal of High Energy Physics*, vol. 2010, no. 11, article 77, pp. 1–31, 2010.
- [43] Z. J. Jiang, H. L. Zhang, J. Wang, K. Ma, and L. M. Cai, “The evolution-dominated hydrodynamics and the pseudorapidity distributions in nucleus-nucleus collisions at low energies at the BNL Relativistic Heavy Ion Collider,” *Chinese Journal of Physics*, Vol. 52, pp. 1676-1685, 2014.